

# A Novel Design of Dielectric Perfect Invisibility Devices

T. Ochiai<sup>1</sup>, U. Leonhardt<sup>2</sup> and J.C. Nacher<sup>3</sup>

February 11, 2008

<sup>1</sup> *Faculty of Engineering, Toyama Prefectural University*

*5180 Kurokawa Imizu-shi Toyama, 939-0398, Japan*

ochiai@pu-toyama.ac.jp

<sup>2</sup> *School of Physics and Astronomy, University of St Andrews*

*North Haugh, St Andrews, KY16 9SS, Scotland*

ulf@st-andrews.ac.uk

<sup>3</sup> *Department of Complex Systems, Future University-Hakodate*

*116-2 Kamedanakano-cho Hakodate, Hokkaido, 041-8655, Japan*

nacher@fun.ac.jp

## Abstract

The aim of an invisibility device is to guide light around any object put inside, being able to hide objects from sight. In this work, we propose a novel design of dielectric invisibility media based on negative refraction and optical conformal mapping that seems to create perfect invisibility. This design has some advantages and more relaxed constraints compared with already proposed schemes. In particular, it represents an example where the time delay in a dielectric invisibility device is zero. Furthermore, due to impedance matching of negatively refracting materials, the reflection should be close to zero. These findings strongly indicate that perfect invisibility with optically isotropic materials is possible. Finally, the area of the invisible space is also discussed.

# 1 Introduction

In Optics, Fermat's principle describes the trajectory of the light as the path taken between two points by light waves that can be traversed in the least time [1, 2]. Each dielectric medium is characterized by a refractive index  $n$ . This index profile integrated along the ray trajectory defines the path length. The value of the refractive index indicates a property of a material that changes the speed of light, computed as the ratio of the speed of light in a vacuum to the speed of light through the material. When light travels at an angle between two different materials, their different refractive indices determine the angle of transmission (refraction) of the ray of light. This relationship is known as Snell's law and illustrates that light changes the trajectory to minimize the time for travel between two points. A well-known example of the optical effect caused by light passing through two media with different refractive indices is a mirage in the desert. The difference in air density changes the refractive indices and makes it possible to see images from the sky above the sand. This is a consequence of the Fermat's Principle, because the light rays follow the shortest path defined by the lowest refractive profiles.

Our invisibility problem has strong links with these principles of Optics. Recently, a few models have been proposed to create a perfect illusion of invisibility. The main idea is to design a dielectric medium composed of a specific refractive index that literally bends and guides the light around a desired object. As the device itself should be invisible, an external observer would not see the object. The optical effect will be equivalent to observe the light rays propagating across empty space, because objects in the background will be visible. Until now, a perfect invisibility effect based on isotropic media has not been achieved and the ultimate wave nature of light has been argued as the main reason. This issue has been extensively debated in several works [3, 4, 5, 6]. However, using anisotropic media these distortions could be reduced to zero, in principle [7]. Furthermore, a recent experimental demonstration of a cloaking device based on artificially structured metamaterials [8] has succeed in decreasing scattered waves emitted from the hidden object. The object remains invisible over a narrow band of microwave frequencies. More recently, a new design of a non-magnetic optical cloak that reduces the scattered waves, and extends the operative range of frequencies to the optical spectrum, was proposed and investigated using computer simulations [9]. Implications of these research lines, future trends and remaining problems on the field are commented and summarized in [10].

The discovery of new materials (also known as *metamaterials*) is opening up exciting avenues for new electromagnetic applications in diverse areas, such as medical imaging, microwaves, lenses, radars, defense and telecommunications. These new features cannot be derived using materials found in nature. Metamaterials then represent artificial media with

unusual electromagnetic properties. These material properties emerge as a consequence of their complex and often periodic structures rather than their chemical composition. Therefore, engineered materials with pre-designed periodic nanostructures could lead to a large range of refractive indices with a rich and great variety of new electromagnetic properties. This is also true for the recently discovered metamaterials with negative refractive index [11]. A striking property of materials with negative index is that the rays will be refracted on the same side of the normal on entering the material according to the Snell's law. The connections between invisibility and negative refraction were described in [12] using the formalism of general relativity.

In this work, we extend the original idea of one of us [5, 6] based on optimal conformal mapping to create dielectric invisibility devices. In this context, we propose a new design for a cloaking device made of a metamaterial with negative refractive index. Our scheme reduces the time delay caused by the device to zero and relaxes the constraints imposed by the requirement for bounded orbits in the Riemann sheet. By following [5, 6], a dielectric medium conformally maps a physical space  $z$  onto Riemann sheets given by an analytic function  $w(z)$ . As a feature of conformal maps, the angles between coordinate lines are conserved. By using, for example, the well-known Joukowski transformation [13, 14], the papers [5, 6] exploit a mapping between the physical space described by the complex field  $z$  and the analytic function  $w(z)$  that represents the mathematical space composed of two Riemann sheets and a branch cut which connects both sheets. As a result any object located at the center of physical space cannot be detected by an external observer. In other words, it seems hidden inside the Riemann sheets.

The most important distortions of invisibility are caused by reflections and time delays [6]. In this work, we investigate how to relax the constraints for designing and manufacturing invisibility devices. In previous works, refractive-index profiles on the interior Riemann sheet should guide the rays around the branch points and should define close loops or trajectories. Therefore, according to classical dynamics [2], the number of potential or index profiles is drastically reduced to a few ones: harmonic-oscillator, Kepler profile and Maxwell's fish eye. In contrast, our proposed design is able to generate a large variety of bounded orbits for rays using striking properties of negative refractive indices. More importantly, the proposed device based on negatively refracting material represents an example where the time delay in a dielectric invisibility device is zero. Furthermore, due to impedance matching of negatively refracting materials the reflection should be close to zero. These findings strongly indicate that perfect invisibility with optically isotropic materials is possible. Finally, the area of the invisible space is also discussed.

## 2 Mathematical Formulation

In this section, we follow refs. [5, 6] and describe the rays of light based on the Hamilton's analogy [1] between the trajectory of rays in media and the motion of particles governed by classical mechanics principles. Let us assume that the refractive index  $n(\mathbf{x})$  does not vary too much comparing with the wavelength of light.

Then, the electromagnetic wave in media can be expressed using the Helmholtz equation:

$$(\Delta + \frac{n^2 \omega^2}{c^2})\psi = 0. \quad (1)$$

Next, we introduce the effective time  $\tau$  measured in spacial units

$$d\tau = \frac{c}{n^2} dt, \quad (2)$$

it is possible to derive the trajectory of rays as follows [2, 5]:

$$\frac{d^2 \mathbf{x}}{d\tau^2} = \frac{1}{2} \nabla n^2. \quad (3)$$

This equation resembles the Newton's second law equation for light rays. Integrated (3) by  $\mathbf{x}$ , we obtain

$$\frac{1}{2} \left( \frac{d\mathbf{x}}{d\tau} \right)^2 - \frac{n^2}{2} = \text{constant}. \quad (4)$$

The corresponding energy  $E$  and potential  $U$  follows the relationship [1, 5]:

$$U - E = -\frac{n^2}{2}. \quad (5)$$

Here, we can show that this constant in the right hand side of (4) vanishes as follows:

$$\frac{1}{2} \left( \frac{d\mathbf{x}}{d\tau} \right)^2 - \frac{n^2}{2} = \frac{1}{2} \left( \frac{dx}{d\tau} \right)^2 - (E - U) = 0. \quad (6)$$

Therefore, from (6) we obtain

$$\left| \frac{d\mathbf{x}}{d\tau} \right| = n. \quad (7)$$

In what follows, we use the Newton's second law equation for light rays (3) for designing invisible devices.

## 3 Conformal mapping

In this section, we review the conformal mapping introduced by [5, 6] in the context of invisibility. This mapping is used to design and create the invisible space inside the material. The property of this conformal mapping and the associated Riemann surfaces plays a crucial role to design the cloaking devices.

### 3.1 Complex plane

We assume that the medium is uniform along the  $z$ -direction. Then, we introduce the complex coordinate  $z = x + iy$  and  $\bar{z} = x - iy$ . The derivative of complex coordinate is given by

$$\frac{\partial}{\partial z} = \frac{1}{2} \left( \frac{\partial}{\partial x} + \frac{1}{i} \frac{\partial}{\partial y} \right), \quad (8)$$

$$\frac{\partial}{\partial \bar{z}} = \frac{1}{2} \left( \frac{\partial}{\partial x} - \frac{1}{i} \frac{\partial}{\partial y} \right). \quad (9)$$

Next, using complex coordinates, Helmholtz equation (1) is transformed into

$$\left( 4 \frac{\partial^2}{\partial z \partial \bar{z}} + \frac{n^2 \omega^2}{c^2} \right) \psi = 0. \quad (10)$$

Let us now consider the analytical function  $w = w(z)$ , which is conformal mapping. Then, by using

$$\frac{\partial}{\partial z} = \frac{\partial w}{\partial z} \frac{\partial}{\partial w} \quad (11)$$

$$\frac{\partial}{\partial \bar{z}} = \frac{\partial \bar{w}}{\partial \bar{z}} \frac{\partial}{\partial \bar{w}}, \quad (12)$$

we find that, by the conformal mapping  $w = w(z)$ , the Laplacian operator is transformed as follows

$$\frac{\partial^2}{\partial z \partial \bar{z}} = \left| \frac{\partial w}{\partial z} \right|^2 \frac{\partial^2}{\partial w \partial \bar{w}}. \quad (13)$$

When the refractive index is transformed as

$$n_z = n_w \left| \frac{dw}{dz} \right| \quad (14)$$

by conformal mapping, the Helmholtz equation (10) is invariant. Here,  $n_z$  and  $n_w$  are the refractive index of  $z$  and  $w$  complex plane, respectively. In what follows, we use this invariance to design the invisible device.

### 3.2 Conformal mapping and Riemann surface

We map the physical space  $z$  into Riemann surface  $w$  by using the following conformal map:

$$w = z + \frac{a^2}{z}. \quad (15)$$

The inverse function of (15) is given by

$$z = \frac{1}{2} (w \pm \sqrt{w^2 - 4a^2}). \quad (16)$$

Here,  $w$ -space is a Riemann surface which consists of two sheets. By the conformal map (15), the outside of the circle  $|z| > a$  is mapped into the first Riemann sheet in  $w$ -space, and the inside of the circle  $|z| < a$  is mapped into the second Riemann sheet in  $w$ -space. The branch cut is given by  $-2a < \text{Re}(w) < 2a, \text{Im}(w) = 0$  in  $w$ -space, which corresponds to the circle  $|z| = a$  in  $z$ -space.

### 3.3 Property of conformal mapping

When we take  $|z| \rightarrow \infty$ , the conformal map (15) is simplified as follows:

$$w \sim z. \quad (17)$$

Therefore, in the asymptotical region  $|z| \rightarrow \infty$ ,  $z$ -space and the first Riemann sheet of  $w$ -space can be identified with each other.

We set  $z$  as polar coordinate  $z = re^{i\theta}$  and  $w$  as cartesian coordinates  $w = u + iv$ , then the conformal map (15) maps the circle ( $r = r_0$ ) in physical  $z$ -space into the ellipse:

$$\frac{u^2}{(a^2/r_0 + r_0)^2} + \frac{v^2}{(a^2/r_0 - r_0)^2} = 1 \quad (18)$$

in  $w$ -space. This property will be used later.

## 4 New model of cloaking devices

### 4.1 Negative-refraction metamaterials

Metamaterials are man-made media where electromagnetic waves do not behave as usually expected. As a consequence, new electromagnetic properties and effects may emerge and be observed. This term is particularly used when the material has properties not found in naturally-formed substances. Therefore, engineered materials with complex and pre-designed nanostructures could lead to a large range of refractive indices with a rich and great variety of new electromagnetic properties in many diverse fields as microelectronics, medical imaging as well as defense and telecommunications [7, 11]. This is also true for the recently discovered metamaterials with negative refractive index. A striking property of materials with negative index is that the rays will be refracted on the same side of the normal on entering the material according to the Snell's law. Then, it allows to use this property to design novel cloaking devices. Here, we propose a device with two Riemann sheets. While the first Riemann sheet the material has refractive index  $n=1$ , the second Riemann sheet is composed of four quadrants with alternative values negative and positive refractive index profile  $n$ . As a consequence, the existence of quadrants with different refractive index makes it possible to generate bounded orbits with more relaxing constrains than suggested previously [5, 6]. By using the negative refractive index, the trajectory around branch cut points in the second Riemann sheet can be seen as a mirror-like reflection of light. We will explain this in detail in the next section.

### 4.2 Refractive index

We first define the refractive index  $n_w$  on Riemann surface  $w$  defined by the conformal mapping (15). We can obtain the refractive index  $n_z$  on

physical space  $z$  by using transformation shown in (14). In what follows, for the matter of convenience, we write just  $n$  for both refractive index  $n_z$  and  $n_w$ , when the meaning is clear from the context.

The space  $w$  is composed by two Riemann sheets. The refractive index of the first Riemann sheet in space  $w$  is given by

$$n_w = 1. \quad (19)$$

Next, we divided the second Riemann sheet in space  $w$  into four regions as follows:

$$\text{Region 1 (R1): } (x < 2a \text{ and } y > 0), \quad (20)$$

$$\text{Region 2 (R2): } (x > 2a \text{ and } y > 0), \quad (21)$$

$$\text{Region 3 (R3): } (x > 2a \text{ and } y < 0), \quad (22)$$

$$\text{Region 4 (R4): } (x < 2a \text{ and } y < 0). \quad (23)$$

The refractive index on the second Riemann sheet in space  $w$  is given by

$$\begin{aligned} n_w &= \sqrt{2E - 2U(x)} \\ &= \begin{cases} \sqrt{2E - 2A(2a - x)} & (\text{R1 : } x < 2a \text{ and } y > 0) \\ -\sqrt{2E + 2A(2a - x)} & (\text{R2 : } x > 2a \text{ and } y > 0) \\ \sqrt{2E + 2A(2a - x)} & (\text{R3 : } x > 2a \text{ and } y < 0) \\ -\sqrt{2E - 2A(2a - x)} & (\text{R4 : } x < 2a \text{ and } y < 0) \end{cases} \quad (24) \end{aligned}$$

These equations implicitly define the potential  $U(x)$  of the Newton equation for the light ray.

It is worth noticing that the refractive index on the second Riemann sheet in space  $w$  is completely antisymmetric with respect to the line  $x = 2a$  and  $x$ -axis.

### 4.3 Energy constraints

Since the value inside the square root in the right hand side of (24) in  $R1$  region should be positive ( $n^2 = 2E - 2U$  should be positive), we obtain the constraint

$$2E > 2A(2a - x). \quad (25)$$

In order to satisfy the previous condition (25) for any starting position on branch cut  $-2a < x < 2a, y = 0$ , we have the constraint

$$E > 4Aa. \quad (26)$$

Therefore, from (26),  $A$  is ranged between

$$0 < A < \frac{E}{4a}. \quad (27)$$

In what follows, we fix the value  $E$ , and consider  $A$  as a free parameter restricted by (27).

#### 4.4 Trajectory of light rays

We will compute the trajectory in  $R1$  region. The other three regions can be obtained by taking a mirror-like reflection of the  $R1$  region. This is the main idea of our approach.

Next, we solve the Newton equation (3) under  $n_w$  given in (24). For the  $R1$  area, the trajectory is given by

$$x = \frac{1}{2}A\tau^2 + v_x\tau + x_0, \quad (28)$$

$$y = v_y\tau. \quad (29)$$

Here,  $v_x$  and  $v_y$  are the initial velocity at the branch cut in second Riemann sheet  $w$  and the absolute value of velocity is given by

$$v_x^2 + v_y^2 = n^2 = 2E - 2A(2a - x_0). \quad (30)$$

The novelty is that, using the negative refractive index, we can enclose the trajectory in the second Riemann sheet in space  $w$  (see Fig. 1). Therefore, we can make the starting point and ending point be the same. Moreover, the direction of initial vector and final vector can coincide with each other.

In contrast, [5, 6] proposed a few examples to enclose the trajectory using bounded orbits according to classical mechanics: Kepler and harmonic-oscillator potentials, and Maxwell's fish eye. We think that our approach is more flexible and admits a large variety of orbits by using the negative index profile features. Thus, it is not limited to the small number of bounded orbits described by classical mechanics.

#### 4.5 The maximum point in the second Riemann sheet

Let  $\tau_1$  be the parameter when the light arrives to the boundary between  $R1$  and  $R2$  area. This can be obtained by solving

$$\frac{1}{2}A\tau_1^2 + v_x\tau_1 + x_0 = 2a. \quad (31)$$

The solution of this equation (31) is given by

$$\tau_1 = \frac{-v_x + \sqrt{v_x^2 + 2A(2a - x_0)}}{A}. \quad (32)$$

From (28), we obtain the minimum  $x$ -point of the parabolic curve in the  $R1$  region as follows

$$x_{min} = -\frac{v_x^2}{2A} + x_0. \quad (33)$$

From (29), the maximum  $y$ -point in  $R1$  region is given by

$$y_{max} = v_y\tau_1 = v_y \frac{-v_x + \sqrt{v_x^2 + 2A(2a - x_0)}}{A}. \quad (34)$$



In what follows, we consider the case that the light enters vertically  $v_x = 0$  for the matter of convenience. Then, (34) becomes

$$y_{max} = 2\sqrt{\left(\frac{E}{A} - (2a - x_0)\right)(2a - x_0)}. \quad (35)$$

We will maximize  $y_{max}$ , by changing the starting point  $x_0$ . This can be done by consider the following two cases (i) and (ii), according to  $A$  value.

(i) In case of  $(\frac{E}{8a} < A < \frac{E}{4a})$

In case of  $(\frac{E}{8a} < A < \frac{E}{4a})$ , (35) takes the maximum

$$y_{max} = \frac{E}{A} \quad (\text{for } \frac{E}{8a} < A < \frac{E}{4a}) \quad (36)$$

when the light ray starts at  $x_0 = 2a - E/(2a)$ .

(ii) In case of  $(0 < A < \frac{E}{8a})$

In case of  $(0 < A < \frac{E}{8a})$ , (35) takes the maximum

$$y_{max} = 4\sqrt{\frac{E}{A}a - 4a^2} \quad (\text{for } 0 < A < \frac{E}{8a}) \quad (37)$$

when the light ray starts at  $x_0 = -2a$ . This starting point is the left hand end point of the branch cut.

In both cases (i) and (ii), with increasing  $A$ ,  $y_{max}$  in space  $w$  decreases, and the invisible space of  $z$  becomes larger. We will discuss this issue in more detail in section 7.

## 5 Time delay

Due to the opposite signs in the refraction index described in the second Riemann sheet, the proposed media presents by construction an example where the time delay in a dielectric invisibility device is zero. In particular, it applies to devices based on optically isotropic materials.

The time delay is conformal invariant and can be computed by

$$\begin{aligned} cT &= \int n_z |dz| \\ &= \int n_w |dw|. \end{aligned} \quad (38)$$

Here, we compute the time delay. First, we focus on the  $R1$  region. Then, the time delay for  $R1$  region is given by

$$\begin{aligned} cT_{R1} &= \int_{C_1} n_w |dw| \\ &= \int_0^{\tau_1} n_w^2 d\tau \\ &= \frac{1}{3}A^2\tau_1^3 + Av_x\tau_1^2 + (2E - 2A(2a - x_0))\tau_1, \end{aligned} \quad (39)$$

where  $C_1$  is the trajectory of the light in R1 region. Inserting (32) into this equation (39), we obtain an explicit form as follows

$$cT_{R1} = (2E - \frac{2}{3}v_x^2 - \frac{4}{3}A(2a - x_0)) \frac{-v_x + \sqrt{v_x^2 + 2A(2a - x_0)}}{A} + \frac{2}{3}v_x(2a - x). \quad (40)$$

We consider the other regions. The time delay on R2 region is the same absolute value as on R1 region but with opposite sign, because the refractive index on R2 has the opposite sign of that on R1,

$$cT_{R1} = \int_{C_1} n_w |dw| = - \int_{C_2} n_w |dw| = -cT_{R2} \quad (41)$$

where  $C_2$  is the trajectory of the light in R2 region.

Similary, for R3 and R4 region, we obtain,

$$cT_{R3} = \int_{C_3} n_w |dw| = - \int_{C_4} n_w |dw| = -cT_{R4} \quad (42)$$

where  $C_3$  and  $C_4$  are the trajectories of the light in R3 and R4 region respectively.

Therefore the total of them is completely cancelled out, and the total time delay is exactly zero.

$$\begin{aligned} cT_{total} &= cT_{R1} + cT_{R2} + cT_{R3} + cT_{R4} \\ &= 0 \end{aligned} \quad (43)$$

## 6 Reflection

Together with time delay, reflection waves are also a distortion that prevents to achieve a perfect invisibility device. However, in the proposed device, due to impedance matching of negatively refracting materials, the reflection should be close zero. This finding, together with the zero time delay shown in the above section, strongly indicates that perfect invisibility is possible in isotropic media.

New materials called metamaterials have recently been created. They are characterized by a negative refractive index. These materials can provide a total refraction phenomena when the wave impedances of the two media are matched. As a consequence, there is no reflected wave, and the distortions due to reflection are zero. Our proposed invisibility device consists of a plane with positive/negative  $n$  boundary. In this case, the reflection would be close to zero by impedance matching. To be precise, given two materials with a defined border, impedance matching means that  $Z_{in}=Z_{out}$  i.e., output impedance of a source of waves is equal to the input impedance of the waves, and there is no reflected wave [15].

Furthermore, it is worth noticing that our case does not contradict Nachman's theorem about the impossibility of perfect invisibility in standard isotropic materials, because these negatively refracting materials exploit the polarized nature of electromagnetic waves. It means that these

materials are described in terms of the permittivity  $\epsilon$  and the permeability  $\mu$ .

Let us illustrate the above described reflectionless property of our proposed device using an incident plane wave solution of Maxwell's equation propagating through a planar dielectric interface.

Let us first consider the reflection coefficients that can be obtained from Maxwell eqs. and the boundary conditions at dielectric interfaces (see [15] for details). In case that  $E$  is vertical to the incoming plane the coefficient reads as

$$\frac{E_r}{E_i} = \frac{\sqrt{\frac{\mu'}{\epsilon'}} \cos \phi - \sqrt{\frac{\mu}{\epsilon}} \sqrt{1 - (\frac{n}{n'})^2 \sin^2 \phi}}{\sqrt{\frac{\mu'}{\epsilon'}} \cos \phi + \sqrt{\frac{\mu}{\epsilon}} \sqrt{1 - (\frac{n}{n'})^2 \sin^2 \phi}}, \quad (44)$$

where  $\phi$  denotes the angle of incidence. In case that  $E$  is parallel to the incoming plane the coefficient is given by

$$\frac{E_r}{E_i} = \frac{\sqrt{\frac{\mu}{\epsilon}} \cos \phi - \sqrt{\frac{\mu'}{\epsilon'}} \sqrt{1 - (\frac{n}{n'})^2 \sin^2 \phi}}{\sqrt{\frac{\mu}{\epsilon}} \cos \phi + \sqrt{\frac{\mu'}{\epsilon'}} \sqrt{1 - (\frac{n}{n'})^2 \sin^2 \phi}}. \quad (45)$$

For a general angle of  $E$ , one should consider linear combination of these two cases. There are three limiting cases (1), (2) and (3):

(1)  $\epsilon = -\epsilon'$  and  $\mu = -\mu'$  case. In this case, there is negative refraction and no reflection at all for a general angle of incidence and polarization:

$$\frac{E_r}{E_i} = 0. \quad (46)$$

We remark that this holds for any polarization, by considering the linear combination of the two cases (i)  $E$  is parallel to incoming plane and (ii)  $E$  is vertical to incoming plane.

(2) Normal incidence case. In this case, the coefficient reads as

$$\frac{E_r}{E_i} = \frac{\sqrt{\frac{\mu}{\epsilon}} - \sqrt{\frac{\mu'}{\epsilon'}}}{\sqrt{\frac{\mu}{\epsilon}} + \sqrt{\frac{\mu'}{\epsilon'}}} = \frac{Z_2 - Z_1}{Z_2 + Z_1}. \quad (47)$$

(3) Impedance-matched case. When  $Z = Z'$ , the coefficient reads as

$$\frac{E_r}{E_i} = \frac{\cos \phi - \sqrt{1 - (\frac{n}{n'})^2 \sin^2 \phi}}{\cos \phi + \sqrt{1 - (\frac{n}{n'})^2 \sin^2 \phi}}. \quad (48)$$

In our problem, at the boundary of R1 and R2, we can take the following form, i.e., case(1):

$$\epsilon_{R1} = -\epsilon_{R2} \quad (\text{at the boundary between R1 and R2}) \quad (49)$$

$$\mu_{R1} = -\mu_{R2} \quad (\text{at the boundary between R1 and R2}) \quad (50)$$

where  $\epsilon_{R1}$  and  $\epsilon_{R2}$  are the permittivity of R1 and R2 region respectively,  $\mu_{R1}$  and  $\mu_{R2}$  are the permeability of R1 and R2 region respectively. This gives the property

$$n_{R1} = -n_{R2} \quad (\text{at the boundary between R1 and R2}) \quad (51)$$

where  $n_{R1}$  and  $n_{R2}$  are the refractive indexes of R1 and R2 regions, respectively. This reproduces the property (24) of our refractive index at the boundary.

In this case, there is no reflection at all for a general angle of incidence and polarization between the boundary of R1 and R2. In the same way, we can show that there is no reflection between the boundary of R2 and R3 (R3 and R4).

As for the branch cut, when vertical entering ( $\phi = 0$ ) in the case of impedance matching ( $Z_1 = Z_2$ ), there is no reflection at the branch cut, see case (2). Otherwise, there is some reflection, because of the discontinuous behavior of refractive index  $n$  and  $n'$ , see case (3). However, in order to achieve perfect invisibility, we can solve this problem by modifying our potential  $U(x)$  as follows. Due to the striking property of negative refracting index, the only requirement for potential  $U(x)$  in R1 region of the second Riemann sheet is that the light should be bent to the left to the right (i.e., the light entering from the first Riemann sheet to R1 region of the second Riemann sheet across the branch cut ( $-2a < x < 2a, y = 0$ ) should go through the boundary between R1 and R2 sheet ( $x = 2a, y > 0$ )). Our potential is the simple example satisfying this condition. However, it is easy to see that there are many other suitable potentials as well. Therefore, we could slightly modify our potential around the branch cut in R1 region to smoothly connecting the potential of the first Riemann sheet to the potential of R1 region, keeping the condition that the light should be bent from the left to the right. Then, the refractive index can be smoothly connected. As a result, there is vanishing reflection around the branch cut at all.

We would like to remark two points. The first remark is that this is possible because our proposed design is flexible enough to potentially generate a large variety of bounded orbits for light rays using the properties of negative refracting indices. The second remark is that this modification does not change the absence of time delay in our device. In other words, even if we modify the potential, the time delay is still zero.

To summarize, we can conclude that perfect invisibility devices in isotropic media seem possible.

## 7 The size of the invisible space

In this section, we investigate the maximum size of invisible space. An object within the size of this space would be invisible and hidden from sight.

### 7.1 The radius of invisible space

Although several local invisible areas may exist, depending on the ray light trajectories, we focus on identifying the symmetric size of invisible

space characterized by radius  $R$ .

From (18), the condition that the  $r < R$  in physical space  $z$  is invisible is as follows. For all point  $(u, v)$  of the ray light trajectory in  $w$ -space, the following equation

$$\frac{u^2}{(a^2/R + R)^2} + \frac{v^2}{(a^2/R - R)^2} < 1 \quad (52)$$

holds. Therefore, the radius of the invisible space is given by the minimum of

$$r = \frac{1}{2\sqrt{2}} \{ \sqrt{u^2 + v^2 + 4a^2} + \sqrt{(u^2 + v^2 + 4a^2)^2 - 16a^2u^2} - \sqrt{u^2 + v^2 - 4a^2} + \sqrt{(u^2 + v^2 - 4a^2)^2 - 16a^2u^2} \} \quad (53)$$

for all points  $(u, v)$  of the ray light trajectory

The possible points for minimizing (53) are  $(u, v) = (2a, y_{max})$  or  $(0, 6a)$ , where  $y_{max}$  is given by (36) and (37).

We will compute these points by considering the following three cases (i), (ii) and (iii), respectively.

(i) In case of  $(u, v) = (2a, y_{max})$  and  $(0 < A < \frac{E}{8a})$ .

By substituting  $u = 2a$  and  $v = y_{max}$  into (53), we transform (53) into

$$r_1(A) = \frac{y_{max}}{4} \{ 1 + \sqrt{1 + \frac{16a^2}{y_{max}^2}} - \sqrt{2 + 2\sqrt{1 + \frac{16a^2}{y_{max}^2}}} \}. \quad (54)$$

Then, substituting (37) into (54), we obtain

$$r_1(A) = \sqrt{\frac{E}{A}} a - 4a^2 \{ 1 + \sqrt{1 + \frac{aA}{E - 4aA}} - \sqrt{2 + 2\sqrt{1 + \frac{aA}{E - 4aA}}} \}. \quad (55)$$

In particular, when  $A \rightarrow 0$

$$r_1(A) \sim \frac{\sqrt{A}}{4\sqrt{E}} a^{\frac{3}{2}}. \quad (56)$$

Thus, when  $A$  is small, the radius of invisible space goes to 0.

(ii) In case of  $(u, v) = (2a, y_{max})$  and  $(\frac{E}{8a} < A < \frac{E}{4a})$ .

Substituting (36) into (54), we obtain

$$r_2(A) = \frac{E}{4A} \{ 1 + \sqrt{1 + \frac{16a^2A^2}{E^2}} - \sqrt{2 + 2\sqrt{1 + \frac{16a^2A^2}{E^2}}} \}. \quad (57)$$

In particular, this function takes the maximum

$$r_2\left(\frac{E}{4a}\right) = (1 + \sqrt{2} - \sqrt{2 + 2\sqrt{2}})a \sim 0.21a, \quad (58)$$

when  $A = \frac{E}{4a}$ .

As an example, we write the value of  $r_2$  for different value of  $A$ . When  $A = \frac{E}{8a}$ ,

$$r_2\left(\frac{E}{8a}\right) = (2 + \sqrt{5} - 2\sqrt{2 + \sqrt{5}})a \sim 0.12a \quad (59)$$

which is smaller than Eq. (60).

(iii) In case of  $(u, v) = (6a, 0)$

By substituting  $(u, v) = (6a, 0)$  into (53), we obtain

$$r_3 = (3 - 2\sqrt{2}) = 0.17a. \quad (60)$$

By summarizing (i), (ii) and (iii), we obtain the radius of the invisible space  $R$  as follows:

$$R(A) = \begin{cases} r_1(A) & (\text{for } 0 < A < \frac{E}{8a}) \\ r_2(A) & (\text{for } \frac{E}{4a} < A < \frac{3E}{16a}) \\ r_3 & (\text{for } \frac{3E}{16a} < A < \frac{E}{4a}), \end{cases} \quad (61)$$

where  $r_1(A)$ ,  $r_2(A)$  and  $r_3$  are given by (55), (57) and (60). Here, we use the fact that  $(r_2(\frac{3E}{16a}) = r_3)$ . We show the radius of the invisible space (61) in Fig. 2. This result indicates that with increasing  $A$ , the radius of invisible space increases up to  $0.17a$ . As the size of the invisible space is proportional to the branch cut  $a$ , the proposed invisibility device may potentially allow us to hide extensive objects.

## 8 Summary

In this work, we have proposed a new design for a cloaking device made of a metamaterial with negative refractive index. Our results indicate that by using negative refractive materials, the constraints for designing and manufacturing invisibility devices can be more relaxed. In previous works, refractive-index profiles on the interior Riemann sheet should guide the rays around the branch points and should define close loops or trajectories. Therefore, according to classical dynamics [2], the number of potential or index profiles was strongly reduced to a few ones: harmonic-oscillator, Kepler profile and Maxwell's fish eye. In contrast, our proposed design is flexible enough to potentially generate a large variety of bounded orbits for light rays using striking properties of negative refractive indices.

More importantly, our device based on optically isotropic material with negatively refracting index represents an example where the time delay is zero. Furthermore, due to impedance matching of negatively refracting materials, the waves are completely transmitted when crossing different material index borders, and reflecting waves are close to zero. These results strongly indicate that perfect invisibility with isotropic materials is possible.

We believe that our proposed design may stimulate theoretical and practical studies for designing and manufacturing cloaking devices using

the properties of negative refraction index. Emerging research based on metamaterials has opened up new avenues by exploiting the artificial dielectric media. From telecommunications, radar and optical invisibility in defense areas to medical imaging and microelectronics in industrial sectors, the new emergent electromagnetic features obtained using metamaterials can bring exciting scientific progress. Further progress toward three-dimensional variations of this scheme is encouraged together with experimental work based on cloaking devices for achieving invisibility in the visible range of the spectrum.

## References

- [1] M. Born and E. Wolf, *Principles of Optics* (Cambridge University Press, Cambridge, 1999).
- [2] L.D. Landau and E.M. Lifshitz, *Mechanics* (Pergamon, Oxford, 1976).
- [3] A. I. Nachman, Ann. Math. **128**, 531 (1998).
- [4] E. Wolf and T. Habashy, J. Mod. Opt. **40**, 785 (1993).
- [5] U. Leonhardt, Science **312**, 1777 (2006).
- [6] U. Leonhardt, New. J. Phys. **8**, 118 (2006).
- [7] J.B. Pendry, D. Schuring and D.R. Smith, Science **312**, 1780 (2006).
- [8] D. Schurig, J. J. Mock, B. J. Justice, S. A. Cummer, J. B. Pendry, A. F. Starr, and D. R. Smith, Science **314**, 977 (2006).
- [9] W.S. Cai, U.K. Chettiar, A.V. Kildishev and V.M. Shalaev, Nature Photonics **1**, 224 (2006).
- [10] U. Leonhardt, Nature Photonics **1**, 207, (2007).
- [11] G.V. Eleftheriades and K.G. Balmain, *Negative-refraction metamaterials* (Wiley Inter-Science, 2006).
- [12] U. Leonhardt, T.G. Philbin, New J. Phys. **8**, 247 (2006).
- [13] Z. Nehari, *Conformal mapping*, (Dover Publications, Inc. New York, 1952).
- [14] L.I. Volkovyskii, G.L. Lunts and I.G. Aramanovich, *A collection of problems on complex analysis* (Dover Publications, Inc. New York, 1965).
- [15] J.D. Jackson, *Classical Electrodynamics* (Wiley, New York, 1999).

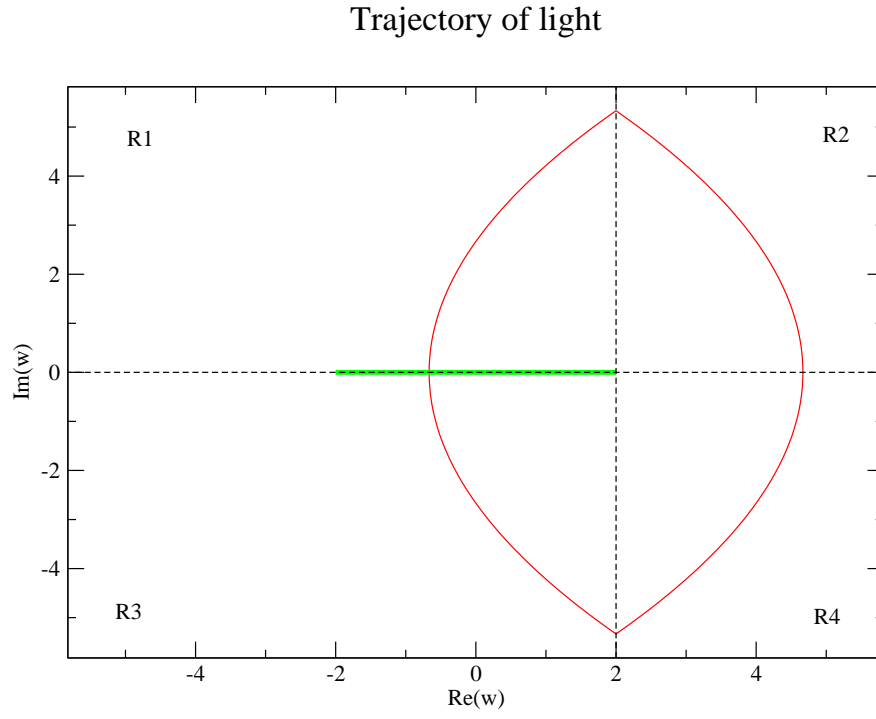


Figure 1: Trajectory of light rays on the second Riemann sheet in space  $w$ . The branch is represented by a bold line between -2 to 2 in the real axis. The four areas describing the refractive index profile of the cloaking device are shown in the figure. Parameters are set to  $a = 1$ ,  $E = 4$ .



The maximum radius of invisible space

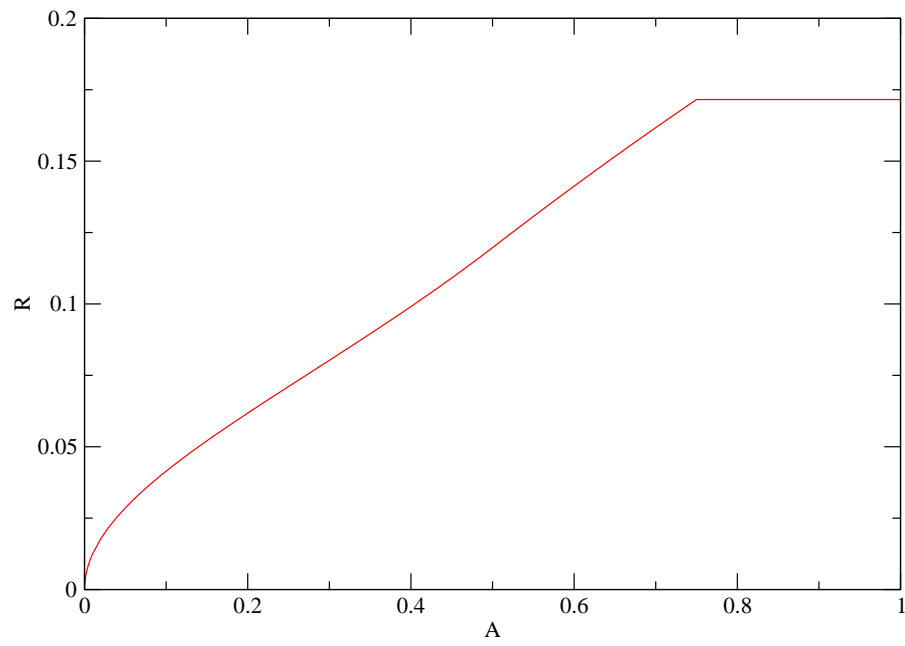


Figure 2: Maximum radius of invisible space. With increasing the potential parameter  $A$ , the radius of invisible space becomes large up to the value  $0.17a$ . Parameters are set to  $a = 1$ ,  $E = 4$ .